



The chemodiversity of algal dissolved organic matter from lysed *Microcystis aeruginosa* cells and its ability to form disinfection by-products during chlorination

Michael Gonsior^{a,*}, Leanne C. Powers^a, Ernest Williams^b, Allen Place^b, Feng Chen^b, Alexander Ruf^{c,d,e}, Norbert Hertkorn^c, Philippe Schmitt-Kopplin^{c,d}

^a University of Maryland Center for Environmental Science, Chesapeake Biological Laboratory, Solomons, USA

^b University of Maryland Center for Environmental Science, Institute of Marine and Environmental Technology, Baltimore, USA

^c Helmholtz Zentrum Muenchen, Research Unit Analytical BioGeoChemistry, Neuherberg, Germany

^d Technische Universität München, Chair of Analytical Food Chemistry, Freising-Weihenstephan, Germany

^e Université Aix-Marseille, Laboratoire de Physique des Interactions Ioniques et Moléculaires (PIIM), UMR CNRS 7345, 13397, Marseille, France

ARTICLE INFO

Article history:

Received 16 October 2018

Received in revised form

21 January 2019

Accepted 9 February 2019

Available online 27 February 2019

Keywords:

Microcystis aeruginosa

Disinfection by-products

FT-ICR MS

Non-target screening

Algal DOM

ABSTRACT

Algal-derived dissolved organic matter (ADOM) originating from lysed *Microcystis aeruginosa* cells was investigated as precursor material to form disinfection by-products upon disinfection with free chlorine. Non-targeted ultrahigh resolution 12 T negative mode electrospray ionization Fourier transform ion cyclotron resonance mass spectrometry (FT-ICR MS) revealed high molecular diversity in solid-phase extracted and ionizable components of *Microcystis aeruginosa* ADOM. The toxin microcystin LR was effectively degraded by free chlorine, which was expected. However, we found a high diversity of disinfection by-products associated with the addition of free chlorine to the water-soluble and solid-phase extractable fraction of ADOM and of double-bond moieties in abundant and known unsaturated fatty acids. Aromatic DOM precursors were absent from known metabolites of *Microcystis aeruginosa* and no evidence for aromatic disinfection by-products (DBPs) was found, despite N-containing compounds. A large diversification of N-containing molecular formulas was observed after chlorination, which seems indicative for the breakdown and oxidation of larger peptides. Additionally, a diverse group of N-compounds with presumed chloramine functional groups was observed. This study highlights the importance to evaluate ADOM and its ability to form different DBPs when compared to allochthonous or terrestrially-derived DOM.

© 2019 The Author(s). Published by Elsevier Ltd. This is an open access article under the CC BY license (<http://creativecommons.org/licenses/by/4.0/>).

1. Introduction

Chloroform was the first discovered disinfection by-product (DBP) and others followed in the 1970s (Rook, 1974). DBPs have been shown to be cytotoxic, carcinogenic, mutagenic, and to be responsible for miscarriage and also birth defects (Bull et al., 2011; Costet et al., 2012; Savitz et al., 2006; Waller et al., 1998). The known DBPs are largely caused by chlorination reactions, but brominated and iodinated compounds have also been discovered (Hua and Reckhow, 2006; Ichihashi et al., 1999). In recent years, nitrogen-containing DBPs have been added to the DBP list (Bond

et al., 2011; Chuang et al., 2013), and some of these N-DBPs showed a drastically increased toxicity (e.g. N-Nitrosodimethylamine (NDMA)) (Mitch et al., 2003; Wagner et al., 2012).

The first U.S. Environmental Protection Agency (EPA) regulation on DBPs was introduced in 1979 after it was confirmed that chloroform and other DBPs caused toxic effects. Regulations on DBPs were expanded in 1998 and 2006 (EPA, 2006). During the last almost 50 years of DBP research, it was established that dissolved organic matter (DOM) precursors are responsible for the formation of DBPs. Hence, research has been focused on linking specific DBPs to DOM (Ichihashi et al., 1999; Khiari et al., 1996; Zhang and Minear, 2002).

Despite tremendous effort in DBP research, it is still not possible to explain the loss of about 50% of the reactive chlorine after it reacts with DOM (Krasner et al., 2006). This fact seems surprising,

* Corresponding author.

E-mail address: gonsior@umces.edu (M. Gonsior).

but the tremendous complexity of DOM has hampered research and the elucidation of all formed DBPs. Hence, there are remaining challenges to fully understand toxicity of still unknown DBPs and the discovery of new DBPs remains an active field of research to date.

Analytical advances have supplied new approaches and tools to tackle the discovery of unknown DBPs and in particular ultrahigh resolution mass spectrometry has been used to decipher complex organic matrices at the molecular level. Mass spectrometry based non-targeted screening for unknown molecular compositions have been successfully used to investigate the complexity of effluent organic matter (Gonsior et al., 2011b; Tseng et al., 2013), freshwater (Gonsior et al., 2016; Kellerman et al., 2014; Stubbins et al., 2010) and marine DOM (Abdulla et al., 2010; D'Andrilli et al., 2010; Gonsior et al., 2011a; Hurdzan et al., 2008; Koch et al., 2008; Koch et al., 2005; Lechtenfeld et al., 2014; Mopper et al., 2007; Perdue et al., 2010; Timko et al., 2015). Very recently this technique has also been used in DBP research (Gong and Zhang, 2015; Gonsior et al., 2014; Lavonen et al., 2013, 2015; Powers and Gonsior, 2018; Zhai et al., 2014; Zhang et al., 2014). These numerous studies have painted a complex picture of a very diverse suite of DBPs that are waiting to be structurally elucidated. Some studies have already determined exact molecular formulas of hundreds of new DBPs (Gong and Zhang, 2015; Gonsior et al., 2014, 2015; Lavonen et al., 2013, 2015; Luek et al., 2017; Yu et al., 2015; Zhai et al., 2014; Zhang et al., 2012, 2014).

Most studies to date investigated DOM and its linked production of DBP during disinfection with DOM that was largely comprised of allochthonous material often referred to as terrestrially-derived DOM. It still remains uncertain what kind of DBPs can be formed from DOM that is derived from autochthonous material or algal-derived DOM (ADOM). It has been recently shown that ADOM contributes significantly to the precursors that form known DBPs (Goslan et al., 2017; Liao et al., 2015; Tomlinson et al., 2016; Yang et al., 2011). Additionally, the formation of N-DBPs arising from chlorination/chloramination of ADOM have been reported and in particular the formation of organic chloramines (Zhang et al., 2016).

ADOM is a substantial component of the DOM pool during algal blooms (Zhang et al., 2014), which is concerning if toxin-producing cyanobacteria are involved. The spatial extent of toxic algal blooms have been increasing in recent years and microcystin LR is a famous example of an algal toxin that is produced within cells of the cyanobacterium *Microcystis aeruginosa* (Honkanen et al., 1990). This toxin-producing alga has caused numerous drinking water advisories in recent years (Falconer, 1999; Jetoo et al., 2015; Qin et al., 2010). Upon disinfection with free chlorine, the microcystin toxins are effectively degraded (Tsuji et al., 1997), but disinfection also lyses cells, that quickly release more toxins from within the cell (Zhang et al., 2017). Hence, additional cell lysis should be avoided and removal of cells is critical prior to chlorination to avoid the release of toxins into the water. In fact, additional operational changes should be implemented at drinking water treatment facilities to destroy the toxin but also to prevent lysis of these cyanobacteria cells (Westrick et al., 2010). For example, activated carbon can effectively remove microcystins, and it is often used in mitigating problems arising from toxic algal blooms (Dixon et al., 2011; Falconer et al., 1989; Roegner et al., 2014; Zhu et al., 2016), but other treatments have also been applied (Roegner et al., 2014). A recent study modeled the degradation of microcystin LR upon treatment with free chlorine and also UV/chlorine (Duan et al., 2018). A combined approach of activated carbon and chlorination with free chlorine is implemented in most cases. (Himberg et al., 1989). Although chlorination inactivates microcystin LR, little is known about additional disinfection by-products (DBPs) that can be formed as a result of the chlorination

of ADOM. Previous work has largely focused on DBPs formed from terrestrially-derived DOM (refs), with a largely polyphenolic composition and is very different from ADOM (Zhang et al., 2014). Furthermore, most studies on ADOM to date have been focused on evaluating the production of known and regulated DBPs (Tomlinson et al., 2016). This approach is limited because ADOM may have very different precursors and hence may produce very different DBPs that may have not yet been discovered. The risk of ADOM related DBPs has been recently acknowledged (Zong et al., 2015) and warrants a more in depth investigation. The use of non-targeted approaches like high resolution mass spectrometry provides the opportunity to study ADOM related DBPs in a more holistic way.

In this study, non-targeted screening of unknown DBPs that formed during disinfection of ADOM generated from lysed *Microcystis aeruginosa* cells was conducted using negative mode electrospray ionization Fourier transform ion cyclotron resonance mass spectrometry (FT-ICR MS). This non-targeted approach is capable of determining exact molecular formulas of DBPs (Gonsior et al., 2014, 2015; Lavonen et al., 2013) that can then be directly related to ADOM sources. Furthermore, a network approach was used to visualize proposed reaction pathways of hypochlorous acid and DBP precursor molecules.

2. Methods

2.1. Culturing of *Microcystis aeruginosa*

The culture medium to grow *M. aeruginosa* was based on the SN recipe (Waterbury et al., 1986), but was modified to contain no NaCl and organic ingredients (no EDTA and vitamin B₁₂). A *M. aeruginosa* strain LE3 containing high levels of microcystin LR was initially maintained in BG11 medium with added vitamin B₁₂ (utex.org) on a 12 h light/dark cycle at 50 $\mu\text{mol photons cm}^{-2} \text{s}^{-1}$. The media was then changed to the SN recipe, exchanged weekly and cultures were scaled to 1 L prior to harvest after 2 weeks.

2.2. Lysis of cells and chlorination experiments

The cellular fraction of cultured *M. aeruginosa* was collected by centrifugation at 1000 \times g for 10 min. The supernatant was decanted and cell pellets were suspended in 2 mL of deionized water in each centrifuge vial resulting in a total volume of 50 mL. Suspended cells in the 50 mL solution were lysed using a barocycler (Pressure Biosciences) with 30 cycles at 34 k psi for 45 s with 15 s intervals in polypropylene tubes. The media that contained no cells was vacuum-filtered through heat-treated (4 h at 500 °C) 0.7 μm GF/F glass fiber filters (Whatman[®]). Approximately 200 mL of the diluted media sample without cells was reserved and underwent no further treatment (blank sample). 50 mg L⁻¹ heat-treated (500 °C) NaCl (extra pure, Acros chemicals) was added to another 200 mL of initial media solution (NaCl blank). The remaining 1147 mL of the 50 mg L⁻¹ NaCl media solution (no cells) was chlorinated for 3 h using an electrochlorination unit (ChlorMaker salt-water chlorine generator, ControlOMatic, Inc.) to achieve a free chlorine concentration of about 10 mg L⁻¹ (exact free chlorine concentration is given in Table 1). The electrochlorination system was used because commercially available hypochlorite solutions are not sufficiently pure to be used in sensitive mass spectrometric approaches. This 10 mg L⁻¹ free chlorine NaCl media solution was then divided into 3 samples in heat-treated (500 °C) borosilicate bottles, and reacted for 24 h at room temperature. This blank treatment was undertaken to compare with the chlorinated lysate samples and to account for potential halogenated products that might have been caused by organic compounds present in the

Table 1
Free chlorine dose and contact times, dissolved organic carbon (DOC), total dissolved nitrogen (TDN) and exact volumes of solid-phase extracted samples for all sample treatments.

Sample	Treatment	Free chlorine (mg L ⁻¹)	Chlorine contact time (h)	DOC (mg L ⁻¹)	TDN (mg L ⁻¹)	V _{extracted} (mL)
Media blanks (no cells)	No treatment	–	–	2.34 ± 0.04	48.1 ± 0.23	198
	NaCl addition	–	–	2.71 ± 0.04	47.4 ± 0.29	193
	chlorination (T0)	11.8 ± 0.17	0	2.71 ± 0.04	47.4 ± 0.29	–
	chlorination A	11.9 ± 0.22	24	2.22 ± 0.05	91.4 ± 0.47	438
	chlorination B	10.8 ± 0.10	24	1.68 ± 0.04	92.8 ± 0.85	320
	chlorination C	10.4 ± 0.19	24	1.70 ± 0.04	90.6 ± 1.05	389
Lysates	No treatment	–	–	8.26 ± 0.12	1.00 ± 0.14	222
	NaCl addition	–	–	9.38 ± 0.08	1.01 ± 0.13	194
	chlorination (T0)	11.1 ± 0.18	0	9.38 ± 0.08	1.01 ± 0.13	–
	chlorination A	6.81 ± 0.13	24	9.58 ± 0.06	0.87 ± 0.02	230
	chlorination B	6.30 ± 0.13	24	9.64 ± 0.16	0.97 ± 0.16	197
	chlorination C	6.00 ± 0.12	24	9.62 ± 0.26	0.87 ± 0.03	219

media itself. Free chlorine concentrations were determined at the beginning of the experiments and again after 24 h free chlorine contact time using HACH method 8021 (USEPA DPD method for free chlorine) with a HACH auto-analyzer and the HACH free chlorine reagent (10 mL). Standards were generated by diluting a 27.6 ± 0.1 mg L⁻¹ low range chlorine standard solution (HACH) with ultrapure water. For all lysate experiments, solutions were created by adding highly concentrated lysate solution to achieve a concentration of about 10 mg L⁻¹ in pure water, and then samples were filtered through 0.7 µm GF/F glass fiber filters. A lysate blank and NaCl blank were prepared in the same way than the media samples (Table 1), but 50 mg L⁻¹ NaCl was added to one of the two lysate blank solutions. About 650 mL of 50 mg L⁻¹ NaCl solution containing no lysate was then chlorinated for 2 h using the electrochlorination unit to reach a free chlorine concentration of 11.1 mg L⁻¹. This free chlorine containing solution was then divided into three replicates and concentrated lysate solution was added to each replicate to reach final dissolved organic carbon (DOC) concentrations of about 10 mg L⁻¹. Exact concentrations of free chlorine, DOC and total dissolved nitrogen (TDN) are given in Table 1. The lysate was then chlorinated for 24 h and sub-samples were used to analyze the remaining free chlorine, DOC and TDN concentrations and to determine optical properties. The remaining solutions of each replicate sample (media blanks and lysates) were acidified to pH 2 using concentrated HCl and solid phase extracted (described below). Exact extraction volumes of each sample are given in Table 1. The pH during all chlorination experiments was at pH 5, which meant that hypochlorous acid (HOCl) was the predominant reactive species. It cannot be ruled out that other reactive species play a role in chlorination of ADOM during the solid-phase extraction procedure at pH 2, but the contact time at pH 2 was held short and below 1 h.

2.3. Dissolved organic carbon (DOC) and total dissolved nitrogen (TDN) analyses

Subsamples of the untreated and treated lysate and media samples were 0.2 µm filtered (Whatman acetate cellulose syringe filters) and acidified to pH 2.5 using concentrated HCl (Pure, 32% ca. solution in water, Sigma Aldrich) for DOC and TDN analysis. DOC and TDN concentrations were determined using a Shimadzu Total Carbon Analyzer (TOC-V_{CPH} analyzer with TNM-1 unit) with potassium hydrogen phthalate and potassium nitrate as standards, respectively.

2.4. Determination of optical properties of ADOM

All samples were filtered through 0.2 µm Whatman acetate

cellulose syringe filters and then filled into a 1 cm fluorescence cuvette. The cuvette was placed in a Horiba Aqualog system, which is able to simultaneously measure absorbance and fluorescence. For each absorbance (excitation) wavelength, a fluorescence emission spectrum was recorded at 3.28 nm intervals at a fixed range between 220.4 and 596.9 nm and a 5 s integration time to generate excitation-emission matrix spectra (EEMS). Because DOM always fluoresces at longer wavelengths than it absorbs, only emission data from excitation wavelengths 220–550 nm were considered for generating EEM spectra. Rayleigh and Raman scattering signals were removed from all EEM spectra in Matlab[®] using methods described previously (Zepp et al., 2004) and any inner filter effects were corrected using the Aqualog software. EEM spectra were then normalized to the emission at 450 nm of a Starna standard reference 1 ppm quinine sulfate solution in 0.1 M HClO₄ using 0.1 M HClO₄ as the quinine sulfate blank (excitation at 347.5 nm, 3.28 nm emission interval, 5 s integration).

2.5. Solid phase extraction (SPE) of ADOM

To be able to use mass spectrometry, all samples needed to be desalted and we used an established solid-phase extraction (SPE) procedure (Dittmar et al., 2008) using the proprietary polymeric Agilent Bond Elut PPL resin. All sample blanks and chlorinated samples were acidified to pH 2 as described above. These samples were then drawn through clean Teflon tubing (rinsed with pH 2 ultrapure water) and connected to 200 mg Agilent PPL cartridges at a flow rate of ~5 mL/min until sample solutions had passed through the cartridges. After extraction, all cartridges were rinsed with 2 mL 0.1% formic acid water (Sigma Aldrich), dried under N₂, and eluted with 2 mL pure methanol (LC-MS Chromasolv, Sigma Aldrich) into heat-treated (500 °C) amber glass vials. All methanol extracts were stored at -20 °C prior to mass spectrometric analysis. The extraction efficiency was about 10% possibly due to extensive loss of highly polar saccharides and small organic acids, which are too polar to be extracted. However, DBP precursors are expected to be extracted due to the required presence of various degrees of unsaturation or aromaticity in the carbon backbone and hence enhanced hydrophobic or mesophilic interaction with the resin. The results from replicates indicated that the extractable component was very reproducible between samples. Regardless, highly polar DBPs are lost during solid phase extraction and the presented results are only addressing the extractable and ionizable component of ADOM.

2.6. Ultrahigh resolution mass spectrometry

We used ultrahigh resolution mass spectrometry to characterize

ADOM and the possible production of DBPs upon chlorination and a Bruker Solarix 12 T Fourier transform (FT) ion cyclotron resonance (ICR) mass spectrometer. Ionization was achieved using negative ion mode electrospray ionization (ESI⁻). The spray voltage was set to -3.6 kV. The methanolic ADOM sample was diluted with pure methanol (Sigma Aldrich Chromasolv) at a ratio of 1:20 to avoid oversaturation and possible space charge effects in the ion cyclotron resonance trap. The flow rate was held constant at $2 \mu\text{L min}^{-1}$ and 500 scans were averaged. The autosampler was programmed to wash with $600 \mu\text{L}$ (80% MeOH, 20% water) between each run to lower the risk of carryover. Blank methanol samples were run between samples. Mass accuracy was <0.2 ppm and accurate molecular formula assignments were combinatorial based on the following atomic numbers: $^{12}\text{C}_{0-\infty}$, $^1\text{H}_{0-\infty}$, $^{16}\text{O}_{0-30}$, $^{14}\text{N}_{0-10}$, $^{32}\text{S}_{0-2}$, and $^{35}\text{Cl}_{0-5}$, as well as the ^{13}C , ^{34}S and ^{37}Cl isotopologues. More details about accurate formula assignments and post calibration can be found elsewhere (Gonsior et al. 2009, 2011a; Koch et al., 2007). Van Krevelen or elemental diagrams (Dittmar 2008; Flerus et al., 2012; Gonsior et al. 2009, 2011a, 2013; Hertkorn et al., 2008; Kim et al., 2003; Sleighter and Hatcher, 2008) and a modified Kendrick plot (Gonsior et al., 2013; Shakeri Yekta et al., 2012) were used to visualize FT-ICR MS data. Additionally, the aromaticity equivalent (Xc) parameter (Yassine et al., 2014) was used to visualize the saturation stages of presumed chlorinated fatty acids. This Xc is essentially a proxy for the degree of saturation of each annotated molecular formula.

2.7. Mass difference network reconstruction

Theoretical ion masses of the above assigned CHO molecular formulas were used to generate the mass difference network. Theoretical ion masses (nodes) were connected by edges if their mass differences were equal (± 0 ppm) to the theoretical mass differences of ΔHOCl (51.971593 amu). Mass difference networks were visualized using the open-source Gephi software (Yifan Hu layout). This technique has been previously described in greater detail (Tziotis et al., 2011).

3. Results and discussion

The chlorination of water soluble *Microcystis aeruginosa* DOM or ADOM revealed that between 4.3 and 5.1 mg L^{-1} free chlorine was consumed (Table 1) within 24 h. The initial free chlorine concentration was 11.1 mg L^{-1} and initial DOC concentrations ranged

between 8.3 and 9.5 mg L^{-1} C. Changes in DOC and TDN concentrations were minimal during chlorination. ADOM showed a few absorbance features (e.g. peaks at 320 , 440 and 680 nm) that were not present after chlorination (Supplementary Material, Fig. S1A). Absorbance of the media blank also decreased after chlorination (Figs. S1A–B). This result is not surprising because a decrease in absorbance and electron donating capacity of DOM is expected and decreases in absorbance of three DOM isolates from the International Humic Substances Society (Suwannee River Fulvic Acid, Suwannee River Humic Acid, and Pony Lake Fulvic Acid) were also previously observed when reacted with free chlorine (Wenk et al., 2013). EEM spectra revealed 3 distinct fluorescence features with peaks at excitation/emission wavelength pairs of $275/325 \text{ nm}$, $270/450 \text{ nm}$, and a broad peak at $350\text{--}380/420\text{--}480 \text{ nm}$ (Supplementary Material, Figs. S1C and D). Fluorescence signals with large Stokes shifts have typically been attributed to humic-like materials (e.g. $250/450$), but have also been observed in picocyanobacteria DOM (Zhao et al., 2017). It is interesting to note that aromatic compounds and humic material in general typically yields higher DBP formation when compared to non-humic materials (Tak and Vellanki, 2018). Integrated fluorescence normalized to absorbance spectra showed that excitation at 270 nm was most efficient, followed by a peak at 360 nm for algal DOM (Supplementary Material, Figs. S1E and F). These fluorescence features were completely destroyed (below detection limit) after 24 h chlorination (Supplementary Material, Figs. S1E–H), indicating that the compounds responsible for these fluorescence signatures are likely DBP precursors.

The chemodiversity as defined by all assigned molecular formulas of ADOM confirmed the very different nature of ADOM when compared to freshwater or estuarine DOM in van Krevelen space (van Krevelen, 1950) (Fig. 1). This is not surprising given the limited molecular diversity of biomolecules arising from lysed cyanobacteria cells. Abundant features in ADOM were fatty acids and some high intensity nitrogen-containing compounds, which are likely peptides. However, any suggested structures cannot be confirmed by FT-ICR MS alone, because FT-ICR MS does not give any information on structure beyond that what can be inferred from a molecular formula alone. Overall, the majority of assigned formulas have a H/C ratio greater than 1.2 within the analytical window of negative mode ESI FT-ICR MS and indicates that this pool is unlikely to contain substantial aromatic moieties even if aliphatic side chains are present. However, slightly unsaturated compounds (H/C ratios of $1.2\text{--}2$) are present and are rather diverse in the CHO pool.

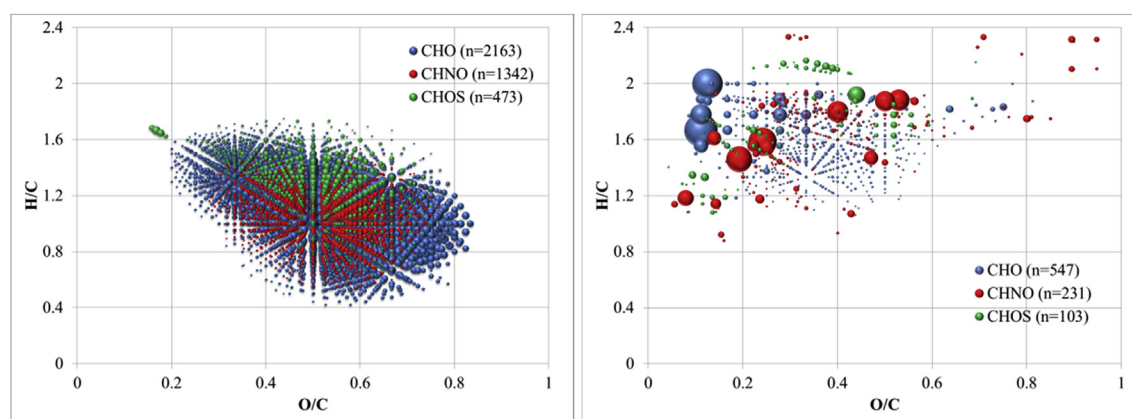


Fig. 1. Chemodiversity of Chesapeake Bay DOM (left) in comparison to ADOM (right) analyzed by negative mode ESI FT-ICR MS. Circle area corresponds to the relative intensity of each m/z ion with CHO in blue, CHNO in red and CHOS in green; van Krevelen diagrams are based on neutral molecular formula assignments. (For interpretation of the references to colour in this figure legend, the reader is referred to the Web version of this article.)

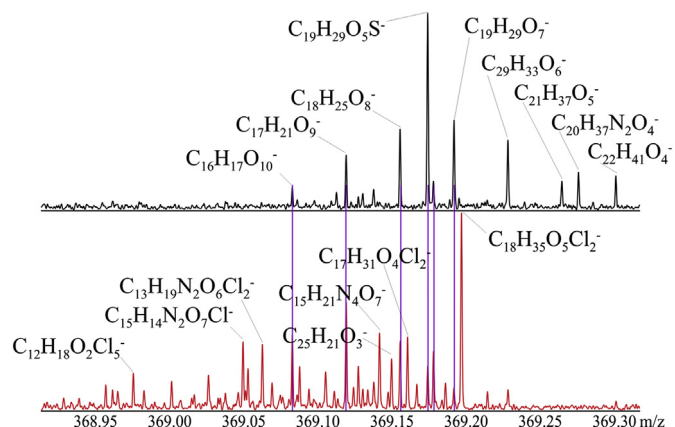


Fig. 2. Ultrahigh resolution negative mode ESI FT-ICR MS of ADOM before and after chlorination zoomed in at nominal mass 369 to demonstrate the high diversity of produced DBPs and the drastic transformation of ADOM in general.

Heteroatomic formulas containing nitrogen or sulfur spanning also a specific range of H/C (1.2–2.2) and O/C (0.1–0.6) ratios in van Krevelen space (Figs. 1 and 3). Within the nitrogen-containing formulas (CHNO), nitrogen-containing aromatic rings may be present at around H/C of 1.2 (e.g. pyrroles with aliphatic side chains),

which might explain the observed fluorescence in ADOM as suggested in a previous study, however this assessment is based on previous work on picocyanobacteria and has not been confirmed using NMR in this study (Zhao et al., 2017).

A large increase in chemodiversity was observed after chlorination and the production of diverse DBPs was demonstrated before and after chlorination. An arbitrary example of the observed differences between mass spectra is given at nominal mass (NM) 369 (Fig. 2). It is clear from the comparison between MS spectra before and after chlorination that ADOM was substantially changed (Figs. 2 and 3), including the complete removal of compounds (i.e. molecular formulas found before chlorination that were not present after chlorination based on formula assignment criteria) and the production of new compounds (i.e. molecular formulas that were not assigned before chlorination). A more in depth direct comparison of non-halogenated compounds showed that all high intensity C_{18} molecular ions containing two oxygen atoms were transformed or degraded upon chlorination (Fig. 3), and the CHO pool decreased in diversity occupying a smaller area within van Krevelen space and fewer formula assignments. Similarly, the highest abundant nitrogen-containing ions were completely degraded, which gives rise to the suggestion that these molecular ions represent peptides, because peptides are effectively degraded upon chlorination, including the microcystin LR toxin itself (Fig. 3). In contrast to the CHO pool, the chemodiversity of CHNO molecular

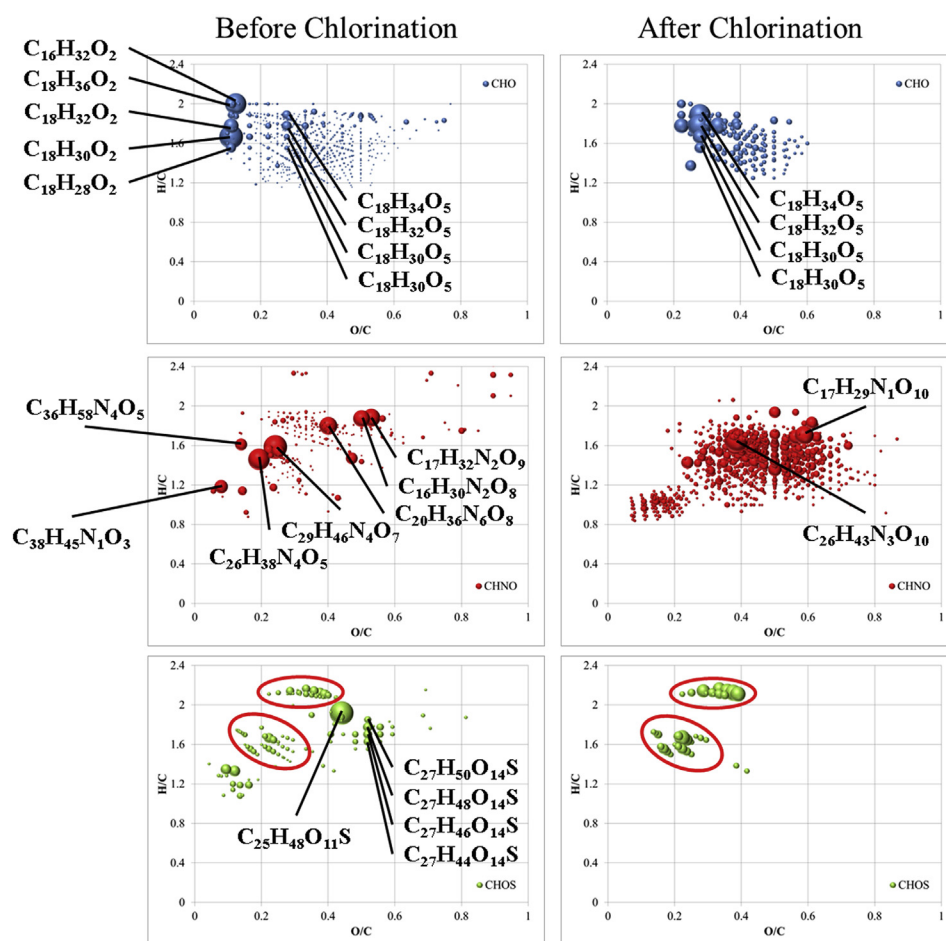


Fig. 3. Van Krevelen diagrams of non-halogenated assigned molecular formulas arising from negative mode ESI FT-ICR MS results before (left panel) and after (right panel) chlorination of ADOM. Circle area corresponds to relative m/z ion peak intensity with **CHO** in blue (top panel), **CHNO** in red (middle panel) and **CHOS** in green (bottom panel); van Krevelen diagrams are based on neutral molecular formulas; red circle indicate potential surface active compounds that are similar to known surfactants. (For interpretation of the references to colour in this figure legend, the reader is referred to the Web version of this article.)

ions dramatically increased from 231 to 1362 assigned molecular formulas. This increase could also indicate the effective degradation of peptides or proteins into smaller molecules upon chlorination. A comparison between the molecular weight before and after chlorination also confirmed the production of complex smaller N-containing m/z ions (Supplementary Material, Fig. S2). Another possible explanation of the extreme diversification of CHNO signatures is that the precursors of the produced CHNO formulas were chemically modified in such a way that they became much more efficient in forming ions during electrospray ionization. All of these newly formed CHNO molecules have to be considered as DBPs. The CHOS signatures that could not be explained with presumably sulfonic acids and surfactants (see red circles, Fig. 3) were also effectively degraded. This comparison between molecular signatures before and after chlorination without the incorporation of chlorine atoms already demonstrated that chlorination transformed the ADOM in a profound way. However, most regulated DBPs are halogenated and the production of organohalides upon disinfection remains a focus in DBP research.

Formula assignments with up to 5 chlorine atoms were assessed to elaborate the production of new chlorinated DBPs arising from chlorination of ADOM. All these assigned chlorine-containing formulas were confirmed using isotope simulation (for an example see Supplementary Material, Fig. S3). The most abundant chlorinated DBPs were assigned to a C_{18} backbone and contained between 1 and 5 chlorine atoms. The most abundant C_{18} -DBPs contained 3 chlorine atoms (Fig. 4), but several C_{18} -DBPs with 2 and 4 chlorines were also observed. C_{18} -DBPs that contained 5 chlorine atoms could be assigned to four specific m/z ions. To visualize the abundance and aromaticity equivalent of all C_{18} molecular formulas, we used van Krevelen and the so-called Xc diagram (Yassine et al., 2014) (Fig. 4). The parameter Xc was previously introduced as a measure for aromaticity and in this case to separate C_{18} compounds of different degree of unsaturation. Different numbers of Xc at any given carbon number (e.g. C_{18}) may indicate different numbers of double bonds, where higher numbers mean a higher degree of double bonds. It can be clearly seen that at carbon number 18 the saturation of double bonds decreased sharply the Xc after chlorination (Fig. 4 Panel B and C), indicative of the addition reaction of free chlorine to double bonds in these presumed fatty acids. Another way to look at changes in saturation is using the carbon oxidation state (COS) of each assigned formula. It can be clearly seen that all molecular formulas with 18 carbon atoms changed to a higher carbon oxidation state including an increase in molecular weight due to the incorporation of chlorine (Supplementary Material, Fig. S4).

These chlorinated C_{18} -DBPs showed the highest intensity in the MS spectra and raised the question about possible precursors. Given the observed complete removal (no m/z ions found in chlorinated samples) of C_{18} molecular ions upon chlorination, and the likely very low degree of aromatic structures within the CHO pool leads to the assumption that only additions of free chlorine on double bonds are viable options for compounds not containing any heteroatoms other than oxygen (CHO compounds only). To test this hypothesis, a mass difference network was computed to probe transformation pathways that represent HOCl addition reactions. In this data-driven analytical approach, nodes represent experimental m/z values and edges (connections within the network) represent exact mass differences, which are equivalent to a net molecular formula of a chemical reaction (Tziotis et al., 2011). Comprehensive chemical reactivity of thousands of different molecules can be studied simultaneously via this approach (Ruf et al., 2017).

Here, this network analysis was performed with C_{18} compounds only as inferred from experimental FT-ICR-MS data. Reaction-equivalent chemical transformations of 1 up to 5 HOCl molecules

with any given $C_{18}HO$ molecular formula present prior chlorination were investigated (Fig. 5). The results indicate that all 42 chlorinated C_{18} -DBPs might be related to the observed 43 $C_{18}HO$ precursors via HOCl addition reactions. In other words, all molecular formulas tested (C_{18} -compounds with and without chlorine) can be related by the transformations or nodes in the network (Fig. 5). We hypothesize that the lost C_{18} precursors are all unsaturated fatty acids of various degrees. It should be noted here that although ESI-FT-ICR MS allows for unambiguous and exact molecular formula assignments, structures cannot be determined due to the unknown number of isomers for any given molecular formula. However, the fatty acid composition of *Microcystis Aeruginosa* is well known and most abundant unsaturated fatty acids are 18:4 ω 3, 18:3 ω 3, 18:3 ω 6 and 18:2 ω 6, which had reported concentrations of 4.95, 4.05, 1.57 and 0.87 mg fatty acids g^{-1} , respectively (Hayakawa et al., 2002), making them the likely C_{18} precursors for the chlorinated C_{18} -DBPs. These fatty acids correspond to the trivial names of stearidonic acid,

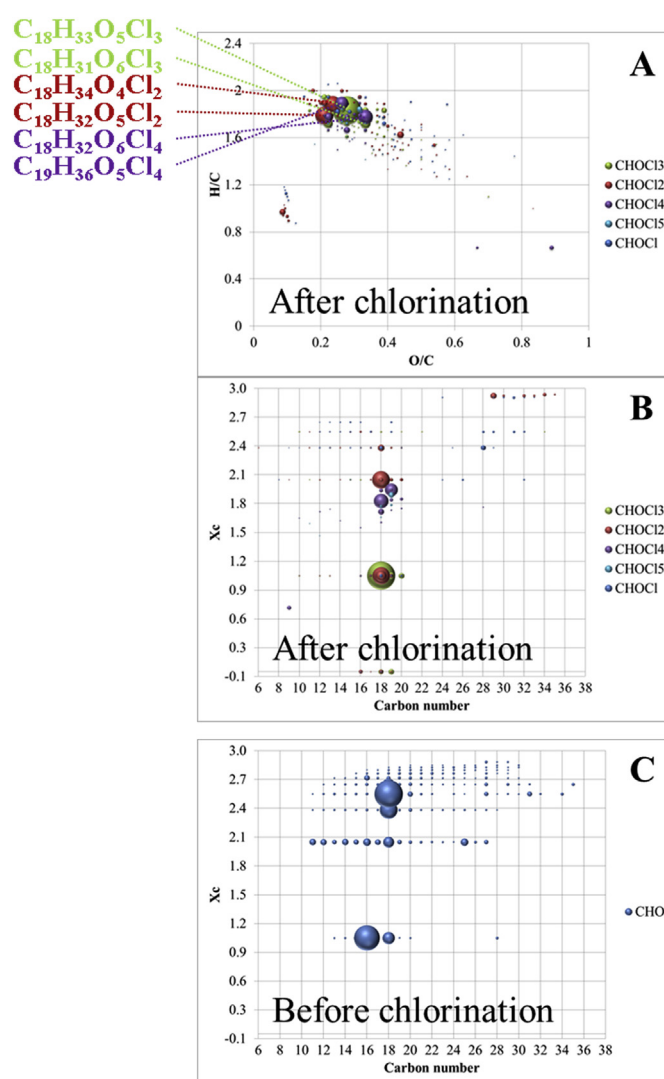


Fig. 4. Chlorinated disinfection by-products produced during chlorination of ADOM and analyzed by negative mode ESI FT-ICR MS (Panel A and B). Formula assignments are based on CHOC1 atoms only. Panel A represents van Krevelen diagrams of produced DBPs according to number of chlorine in each assigned formula. Panel B shows the carbon number of assigned formulas versus the aromaticity Equivalent (Xc) (Yassine et al., 2014) in the chlorinated sample and panel C in the unchlorinated sample, respectively. Note: The highest abundant C_{18} and C_{19} molecular formula assignments are highlighted with exact neutral formulas in Panel A.

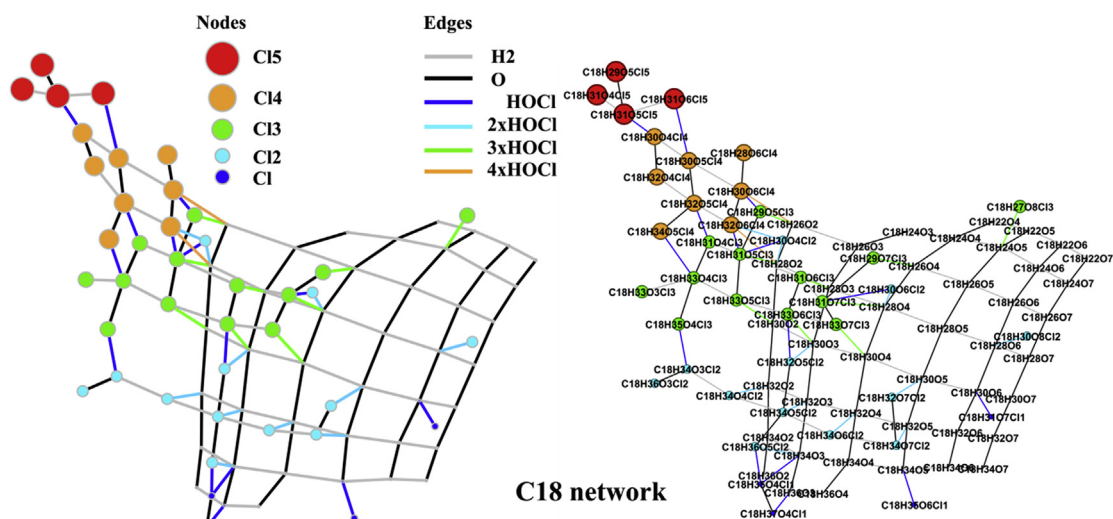


Fig. 5. Mass difference network analysis of all $C_{18}HO$ and $HOCl$ molecular formulas before and after chlorination to show that a simple addition of hypochlorous acid might explain the observed newly described DBPs arising from presumably fatty acid precursors.

α -linolenic acid, γ -linolenic acid and linoleic acid, respectively. All these unsaturated fatty acids are well documented in algal cells and corresponded to the presumed fatty acids that were removed upon chlorination. Thus, we undertook collision induced dissociation MS-MS experiments on three of the proposed fatty acids to confirm structures (Supplementary Material, Fig. S9). Although we cannot determine concentrations of these fatty acids using this approach, the MS-MS spectra of stearidonic, linolenic and linoleic acid matched published spectral records MT000005, MT000072 and MT000114, respectively in the MassBank database (Horai et al., 2010) (Supplementary Material, Fig. S9). A diverse group of hydroxylated unsaturated fatty acids also might be present in ADOM, due to oxidative transformations or via other hydroxylated unsaturated fatty acids that are present in metabolic pathways. Proposed putative reactions of these fatty acids to form chlorinated fatty acid DBPs are given in Supplementary Material (Figs. S5–S7). The presence of additional C_{18} -DBPs indicated their formation via hydroxylated unsaturated fatty acids in the ADOM. 17-hydroxylinolenic acid is known to be involved in α -linolenic acid metabolism. This compound might be an additional precursor for DBPs. Its proposed reaction pathway with $HOCl$ is given in the Supplementary Material (Fig. S8).

Previous studies showed that chlorination of fatty acids is likely due to the reaction with $HOCl$ and not OCl^- (Winterbourn et al., 1992). Furthermore, the addition of single $HOCl$ molecules was not the only reaction observed, but also the addition of 2 chlorine atoms on a single double bond, which is consistent with previous studies (Dembitsky and Srebnik, 2002; Winterbourn et al., 1992). The multiple addition of $HOCl$ on all existing double bonds in unsaturated fatty acids have been shown to be fast and almost stoichiometric (Winterbourn et al., 1992). The presence of chlorinated fatty acids with 5 Cl atoms can only be explained by the addition of two chlorine atoms to at least one double bond of the stearidonic acid (Supplementary online material Fig. S7). We would have found a single addition of $HOCl$ on linolenic or stearidonic acid if a single addition of $HOCl$ would be possible on unsaturated fatty acids containing several double bonds, which was not the case. The mass difference network analysis creates a framework of possible transformation pathways and it took only the addition of $HOCl$ into account (Fig. 5). These results underline the feasibility to explain

the formation of all observed C_{18} -DBPs (Fig. 5). Isotopically labeled $HOCl$ was previously used to trace its incorporation into lipids (Ghanbari et al., 1982) and the authors confirmed two chlorinated products after the reaction of oleic acid and $HO^{36}Cl$. A fast addition of $HOCl$ on fatty acids was also shown in the context of drinking water disinfection (Gibson et al., 1986).

Chlorinated nitrogen-containing DBPs were also confirmed that predominantly showed the incorporation of one chlorine atom, but a few two and three chlorine single molecules were also found (Fig. 6). In total 283 chlorinated N-DBPs were confirmed using isotope simulation (Fig. 6). A very diverse suite of non-halogenated N-DBPs, with a large molecular weight range between 200 Da and 700 Da and an intensity-weighted center of mass of 456.5 were also observed (Fig. 6). No change in the degree of saturation was observed after chlorination as expressed in the Xc diagrams (Fig. 6), which suggests the formation of chloramines rather than any reaction of chlorine on the carbon backbone. The large diversification of unchlorinated N-DBPs might be due to fragmentation of larger peptides or proteins, but this hypothesis remains to be confirmed in future studies.

The newly described DBPs in this study demonstrated the need to describe ADOM-related DBPs in greater detail and the used non-targeted approach demonstrated the existence of a very diverse group of DBPs that are specific to ADOM. Results from this study might be used to address potential toxicity of halogenated fatty acids. Furthermore, the very high diversity of N-DBPs (halogenated and non-halogenated) is equally of concern and should be a focus point of additional studies.

4. Conclusions

Algal-derived DOM from lysed *Microcystis aeruginosa* cells was drastically transformed upon chlorination with free chlorine. No changes in DOC concentration were observed after chlorination, but ADOM absorbance peaks were removed and/or reduced and ADOM fluorescence signals were completely removed (Supplementary Material, Fig. S1). Because only a portion of the entire ADOM absorbs and fluoresces light, non-targeted high resolution mass spectrometry was used to gain molecular level understanding of the changes in ADOM before and after chlorination.

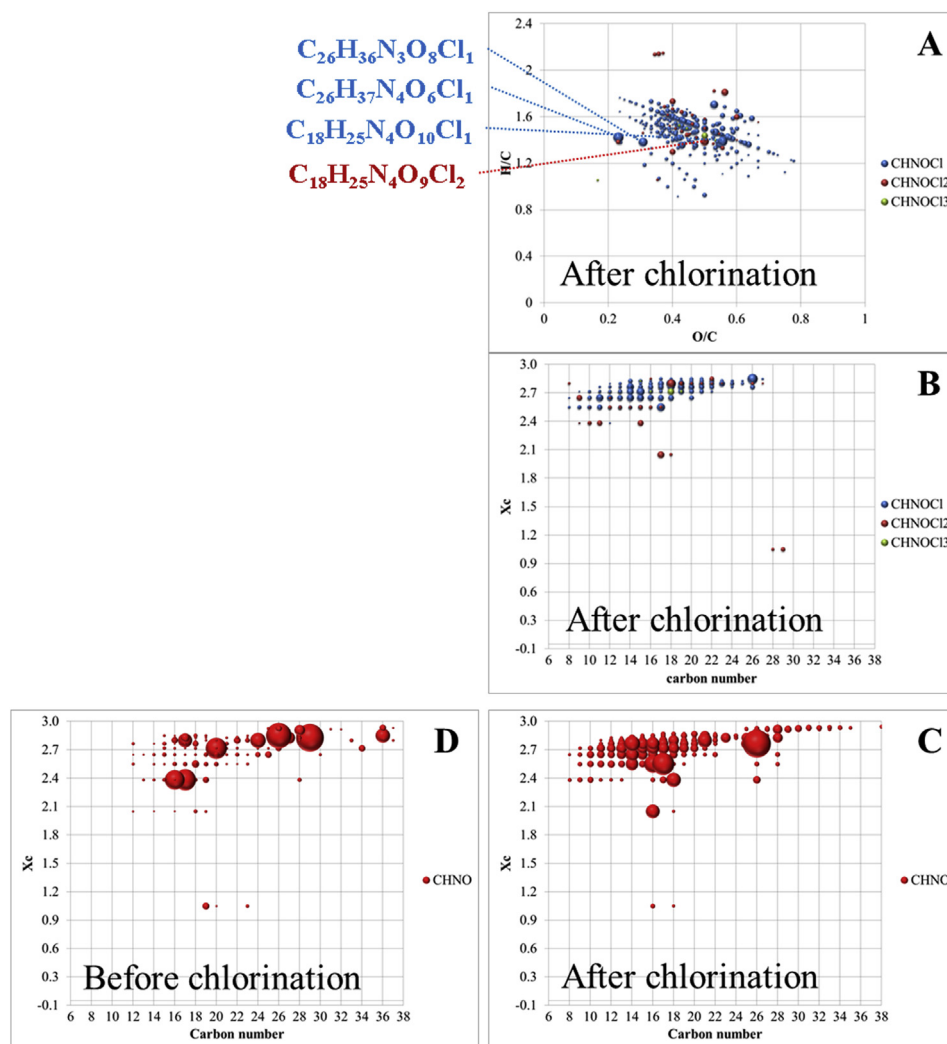


Fig. 6. Chlorinated and non-chlorinated nitrogen-containing disinfection by-products produced during chlorination of ADOM and then analyzed by negative mode ESI and FT-ICR MS. Formula assignments based on CHNOCl atoms only. van Krevelen diagram after chlorination (Panel A); Xc diagram of chlorinated N-DBPs (Panel B) formed after chlorination; Xc diagram of non-chlorinated N-DBPs formed after chlorination; and Xc diagram of N-containing assigned molecular formula before chlorination (Panel D). Note: Most abundant chlorinated DBPs are highlighted with exact neutral molecular formulas in Panel A.

This ADOM showed a chlorination of presumed unsaturated fatty acids containing up to 5 chlorine atoms and could be explained by addition of HOCl to the double bonds in individual fatty acids. Although we could not determine concentrations of these fatty acids in our ADOM sample, which would be critical for determining potential toxicity. Chlorinated fatty acids have been previously confirmed as DBPs in effluent from paper mills that still used chlorination for bleaching (Voss and Rapsomatiotis, 1985; Wesén et al., 1992). Furthermore, diverse suite of halogenated fatty acids have been confirmed to occur naturally and are summarized elsewhere (Dembitsky and Srebnik, 2002). Thus, chlorinated fatty acids warrant further investigation when algal DOM is a major DBP precursor or bloom conditions are present.

The diversity of N-containing DBPs with and without chlorine present increased almost 10-fold and chlorinated N-DBPs might reflect an effective production of complex and high molecular weight chloramines, but their stability remains unknown. A potential anthropogenic source of chlorinated lipids is of interest because they may be involved in inflammatory disease (Spickett, 2007) and has been a focus point in recent years. This study warrants further studies in quantifying halogenated fatty acids and in

understanding the formation of diverse N-DBPs from ADOM and potentially other algal DOM sources.

Acknowledgements

This is contribution 19-009 for IMET and 5562 of the University of Maryland Center for Environmental Science. Financial assistance was obtained from NSF Environmental Chemical Sciences Award # 1708766 to Michael Gonsior.

Appendix A. Supplementary data

Supplementary data to this article can be found online at <https://doi.org/10.1016/j.watres.2019.02.030>.

References

- Abdulla, H.A.N., Minor, E.C., Dias, R.F., Hatcher, P.G., 2010. Changes in the compound classes of dissolved organic matter along an estuarine transect: a study using FTIR and ^{13}C NMR. *Geochem. Cosmochim. Acta* 74 (13), 3815–3838.
- Bond, T., Huang, J., Templeton, M.R., Graham, N., 2011. Occurrence and control of nitrogenous disinfection by-products in drinking water – a review. *Water Res.* 45 (15), 4341–4354.

- Bull, R.J., Reckhow, D.A., Li, X., Humpage, A.R., Joll, C., Hrudehy, S.E., 2011. Potential carcinogenic hazards of non-regulated disinfection by-products: haloquinones, halo-cyclopentene and cyclohexene derivatives, N-halamines, halonitriles, and heterocyclic amines. *Toxicology* 286 (1–3), 1–19.
- Chuang, Y.H., Lin, A.Y.C., Wang, X.H., Tung, H.H., 2013. The contribution of dissolved organic nitrogen and chloramines to nitrogenous disinfection byproduct formation from natural organic matter. *Water Res.* 47 (3), 1308–1316.
- Costet, N., Garlantezec, R., Monfort, C., Rouget, F., Gagniere, B., Chevrier, C., Cordier, S., 2012. Environmental and urinary markers of prenatal exposure to drinking water disinfection by-products, fetal growth, and duration of gestation in the PELAGIE birth cohort (Brittany, France, 2002–2006). *Am. J. Epidemiol.* 175 (4), 263–275.
- D'Andrilli, J., Dittmar, T., Koch, B.P., Purcell, J.M., Marshall, A.G., Cooper, W.T., 2010. Comprehensive characterization of marine dissolved organic matter by Fourier transform ion cyclotron resonance mass spectrometry with electrospray and atmospheric pressure photoionization. *Rapid Commun. Mass Spectrom.* 24, 643–650.
- Dembitsky, V.M., Srebniak, M., 2002. Natural halogenated fatty acids: their analogues and derivatives. *Prog. Lipid Res.* 41 (4), 315–367.
- Dittmar, T., 2008. The molecular level determination of black carbon in marine dissolved organic matter. *Org. Geochem.* 39, 396–407. Copyright (C) 2011 American Chemical Society (ACS). All Rights Reserved.
- Dittmar, T., Koch, B., Hertkorn, N., Kattner, G., 2008. A simple and efficient method for the solid-phase extraction of dissolved organic matter (SPE-DOM) from seawater. *Limnol Oceanogr. Methods* 6 (June), 230–235.
- Dixon, M.B., Richard, Y., Ho, L., Chow, C.W.K., O'Neill, B.K., Newcombe, G., 2011. A coagulation–powdered activated carbon–ultrafiltration – multiple barrier approach for removing toxins from two Australian cyanobacterial blooms. *J. Hazard Mater.* 186 (2), 1553–1559.
- Duan, X., Sanan, T., de la Cruz, A., He, X., Kong, M., Dionysiou, D.D., 2018. Susceptibility of the algal toxin microcystin-LR to UV/chlorine process: comparison with chlorination. *Environ. Sci. Technol.*
- EPA, U.S., 2006. National Primary Drinking Water Regulations: Stage 2 Disinfectants and Disinfection Byproducts Rule, p. 388 (Federal Register).
- Falconer, I.R., 1999. An Overview of problems caused by toxic blue–green algae (cyanobacteria) in drinking and recreational water. *Environ. Toxicol.* 14 (1), 5–12.
- Falconer, I.R., Runnegar, M.T.C., Buckley, T., Van, L.H., Bradshaw, P., 1989. Using activated carbon to remove toxicity from drinking water containing cyanobacterial blooms. *Journal (American Water Works Association)* 81 (2), 102–105.
- Flerus, R., Lechtenfeld, O.J., Koch, B.P., McCallister, S.L., Schmitt-Kopplin, P., Benner, R., Kaiser, K., Kattner, G., 2012. A molecular perspective on the ageing of marine dissolved organic matter. *Biogeosciences* 9 (6), 1935–1955.
- Ghanbari, H.A., Wheeler, W.B., Kirk, J.R., 1982. Reactions of aqueous chlorine and chlorine dioxide with lipids: chlorine incorporation. *J. Food Sci.* 47 (2), 482–485.
- Gibson, T.M., Haley, J., Righton, M., Watts, C.D., 1986. Chlorination of fatty acids during water treatment disinfection: reactivity and product identification. *Environ. Technol. Lett.* 7 (1–12), 365–372.
- Gong, T., Zhang, X., 2015. Detection, identification and formation of new iodinated disinfection byproducts in chlorinated saline wastewater effluents. *Water Res.* 68 (0), 77–86.
- Gonsior, M., Mitchelmore, C., Heyes, A., Harir, M., Richardson, S.D., Petty, W.T., Wright, D.A., Schmitt-Kopplin, P., 2015. Bromination of marine dissolved organic matter following full scale electrochemical ballast water disinfection. *Environ. Sci. Technol.* 49 (15), 9048–9055.
- Gonsior, M., Peake, B.M., Cooper, W.T., Podgorski, D., D'Andrilli, J., Cooper, W.J., 2009. Photochemically induced changes in dissolved organic matter identified by ultrahigh resolution fourier transform ion cyclotron resonance mass spectrometry. *Environ. Sci. Technol.* 43, 698–703.
- Gonsior, M., Peake, B.M., Cooper, W.T., Podgorski, D.C., D'Andrilli, J., Dittmar, T., Cooper, W.J., 2011a. Characterization of dissolved organic matter across the subtropical convergence off the south Island, New Zealand. *Mar. Chem.* 123 (1–4), 99–110.
- Gonsior, M., Schmitt-Kopplin, P., Bastviken, D., 2013. Depth-dependent molecular composition and photo-reactivity of dissolved organic matter in a boreal lake under winter and summer conditions. *Biogeosciences* 10 (11), 6945–6956.
- Gonsior, M., Schmitt-Kopplin, P., Stavklint, H., Richardson, S.D., Hertkorn, N., Bastviken, D., 2014. Changes in dissolved organic matter during the treatment processes of a drinking water plant in Sweden and formation of previously unknown disinfection byproducts. *Environ. Sci. Technol.* 48 (21), 12714–12722.
- Gonsior, M., Valle, J., Schmitt-Kopplin, P., Hertkorn, N., Bastviken, D., Luek, J., Harir, M., Bastos, W., Enrich-Prast, A., 2016. Chemodiversity of dissolved organic matter in the Amazon Basin. *Biogeosciences* 13 (14), 4279–4290.
- Gonsior, M., Zwartjes, M., Cooper, W.J., Song, W., Ishida, K.P., Tseng, L.Y., Jeung, M.K., Rosso, D., Hertkorn, N., Schmitt-Kopplin, P., 2011b. Molecular characterization of effluent organic matter identified by ultrahigh resolution mass spectrometry. *Water Res.* 45 (9), 2943–2953.
- Goslan, E.H., Seigle, C., Purcell, D., Henderson, R., Parsons, S.A., Jefferson, B., Judd, S.J., 2017. Carbonaceous and nitrogenous disinfection by-product formation from algal organic matter. *Chemosphere* 170, 1–9.
- Hayakawa, K., Tsujimura, S., Napolitano, G.E., Nakano, S., Kumagai, M., Nakajima, T., Jiao, C., 2002. Fatty acid composition as an indicator of physiological condition of the cyanobacterium *Microcystis aeruginosa*. *Limnology* 3 (1), 29–35.
- Hertkorn, N., Frommberger, M., Witt, M., Koch, B., Schmitt-Kopplin, P., Perdue, E.M., 2008. Natural organic matter and the event horizon of mass spectrometry. *Anal. Chem.* 80 (23), 8908–8919.
- Himberg, K., Keijola, A.M., Hiisvirta, L., Pyysalo, H., Sivonen, K., 1989. The effect of water treatment processes on the removal of hepatotoxins from *Microcystis* and *oscillatoria* cyanobacteria: a laboratory study. *Water Res.* 23 (8), 979–984.
- Honkanen, R.E., Zwiller, J., Moore, R.E., Daily, S.L., Khatra, B.S., Dukelow, M., Boynton, A.L., 1990. Characterization of microcystin-LR, a potent inhibitor of type 1 and type 2A protein phosphatases. *J. Biol. Chem.* 265 (32), 19401–19404.
- Horai, H., Arita, M., Kanaya, S., Nihei, Y., Ikeda, T., Suwa, K., Ojima, Y., Tanaka, K., Tanaka, S., Aoshima, K., Oda, Y., Kakazu, Y., Kusano, M., Tohge, T., Matsuda, F., Sawada, Y., Hirai, M.Y., Nakanishi, H., Ikeda, K., Akimoto, N., Maoka, T., Takahashi, H., Ara, T., Sakurai, N., Suzuki, H., Shibata, D., Neumann, S., Iida, T., Tanaka, K., Funatsu, K., Matsuura, F., Soga, T., Taguchi, R., Saito, K., Nishioku, T., 2010. MassBank: a public repository for sharing mass spectral data for life sciences. *J. Mass Spectrom.* 45 (7), 703–714.
- Hua, G., Reckhow, D., 2006. Determination of TOCl, TOBr and TOI in drinking water by pyrolysis and off-line ion chromatography. *Anal. Bioanal. Chem.* 384 (2), 495–504.
- Hurdzan, C.M., Basta, N.T., Hatcher, P.G., Tuovinen, O.H., 2008. Phenanthrene release from natural organic matter surrogates under simulated human gastrointestinal conditions. *Ecotoxicol. Environ. Saf.* 69, 525–530. Copyright (C) 2011 American Chemical Society (ACS). All Rights Reserved.
- Ichihashi, K., Teranishi, K., Ichimura, A., 1999. Brominated trihalomethane formation in halogenation of humic acid in the coexistence of hypochlorite and hypobromite ions. *Water Res.* 33 (2), 477–483.
- Jetoo, S., Grover, V.L., Krantzberg, G., 2015. The toledo drinking water advisory: suggested application of the water safety planning approach. *Sustainability* 7 (8), 9787–9808.
- Kellerman, A.M., Dittmar, T., Kothawala, D.N., Tranvik, L.J., 2014. Chemodiversity of dissolved organic matter in lakes driven by climate and hydrology. *Nat. Commun.* 5, 3804.
- Khiari, D., Krasner, S.W., Hwang, C.J., Chinn, R., Barrett, S., 1996. Effects of Chlorination and Chloramination on the Molecular Weight Distribution of Natural Organic Matter and the Production of High-Molecular-Weight Disinfection By-Products. American Water Works Association, Boston, MA.
- Kim, S., Kramer, R.W., Hatcher, P.G., 2003. Graphical method for analysis of ultrahigh-resolution broadband mass spectra of natural organic matter, the van krevelen diagram. *Anal. Chem.* 75 (20), 5336–5344.
- Koch, B.P., Dittmar, T., Witt, M., Kattner, G., 2007. Fundamentals of molecular formula assignment to ultrahigh resolution mass data of natural organic matter. *Anal. Chem.* 79 (4), 1758–1763.
- Koch, B.P., Ludwiczowski, K.-U., Kattner, G., Dittmar, T., Witt, M., 2008. Advanced characterization of marine dissolved organic matter by combining reversed-phase liquid chromatography and FT-ICR-MS. *Mar. Chem.* 111 (3–4), 233–241.
- Koch, B.P., Witt, M., Engbrodt, R., Dittmar, T., Kattner, G., 2005. Molecular formulae of marine and terrigenous dissolved organic matter detected by electrospray ionization Fourier transform ion cyclotron resonance mass spectrometry. *Geochim. Cosmochim. Acta* 69 (13), 3299–3308.
- Krasner, S.W., Weinberg, H.S., Richardson, S.D., Pastor, S.J., Chinn, R., Scimenti, M.J., Onstad, G.D., Thurston, A.D., 2006. Occurrence of a new generation of disinfection byproducts. *Environ. Sci. Technol.* 40 (23), 7175–7185.
- Lavonen, E.E., Gonsior, M., Tranvik, L.J., Schmitt-Kopplin, P., Köhler, S.J., 2013. Selective chlorination of natural organic matter: identification of previously unknown disinfection byproducts. *Environ. Sci. Technol.* 47 (5), 2264–2271.
- Lavonen, E.E., Kothawala, D.N., Tranvik, L.J., Gonsior, M., Schmitt-Kopplin, P., Köhler, S.J., 2015. Tracking changes in the optical properties and molecular composition of dissolved organic matter during drinking water production. *Water Res.* 85, 286–294.
- Lechtenfeld, O.J., Kattner, G., Flerus, R., McCallister, S.L., Schmitt-Kopplin, P., Koch, B.P., 2014. Molecular transformation and degradation of refractory dissolved organic matter in the Atlantic and Southern Ocean. *Geochim. Cosmochim. Acta* 126 (0), 321–337.
- Liao, X., Liu, J., Yang, M., Ma, H., Yuan, B., Huang, C.-H., 2015. Evaluation of disinfection by-product formation potential (DBFPF) during chlorination of two algae species — blue-green *Microcystis aeruginosa* and diatom *Cyclotella meneghiniana*. *Sci. Total Environ.* 532, 540–547.
- Luek, J.L., Schmitt-Kopplin, P., Mouser, P.J., Petty, W.T., Richardson, S.D., Gonsior, M., 2017. Halogenated organic compounds identified in hydraulic fracturing wastewaters using ultrahigh resolution mass spectrometry. *Environ. Sci. Technol.* 51 (10), 5377–5385.
- Mitch, W.A., Sharp, J.O., Trussell, R.R., Valentine, R.L., Alvarez-Cohen, L., Sedlak, D.L., 2003. N-nitrosodimethylamine (NDMA) as a drinking water contaminant: a review. *Environ. Eng. Sci.* 20 (5), 389–404.
- Mopper, K., Stubbins, A., Ritchie, J.D., Bialk, H.M., Hatcher, P.G., 2007. Advanced instrumental approaches for characterization of marine dissolved organic matter: extraction techniques, mass spectrometry, and nuclear magnetic resonance spectroscopy. *Chem. Rev.* 107 (2), 419–442.
- Perdue, E.M., Green, N.W., Chen, H., Stubbins, A., Mopper, K., Mao, J., Helms, J.R., Hatcher, P.G., 2010. Chemical and Spectroscopic Characterization of Marine Dissolved Organic Matter Isolated Using the Coupled Reverse Osmosis-Electrodialysis (RO/ED) Method. American Chemical Society. GEOC-137.
- Powers, L., Gonsior, M., 2018. Non-targeted screening of disinfection by-products in desalination plants using mass spectrometry: a review. *Current Opinion in Environm. Sci. Health.*
- Qin, B., Zhu, G., Gao, G., Zhang, Y., Li, W., Paerl, H.W., Carmichael, W.W., 2010.

- A drinking water crisis in lake taihu, China: linkage to climatic variability and lake management. *Environ. Manag.* 45 (1), 105–112.
- Roegner, A.F., Brena, B., Gonzalez-Sapienza, G., Puschner, B., 2014. Microcystins in potable surface waters: toxic effects and removal strategies. *J. Appl. Toxicol.* 34 (5), 441–457.
- Rook, J.J., 1974. Formation of haloforms during chlorination of natural waters. *Water Treat. Exam.* (23), 234–243.
- Ruf, A., Kanawati, B., Hertkorn, N., Yin, Q.-Z., Moritz, F., Harir, M., Lucio, M., Michalke, B., Wimpenny, J., Shilobreeva, S., Bronsky, B., Saraykin, V., Gabelica, Z., Gougeon, R.D., Quirico, E., Ralew, S., Jakubowski, T., Haack, H., Gonsior, M., Jenniskens, P., Hinman, N.W., Schmitt-Kopplin, P., 2017. Previously unknown class of metalorganic compounds revealed in meteorites. *Proc. Natl. Acad. Sci. Unit. States Am.* 114 (11), 2819–2824.
- Savitz, D.A., Singer, P.C., Herring, A.H., Hartmann, K.E., Weinberg, H.S., Makarushka, C., 2006. Exposure to drinking water disinfection by-products and pregnancy loss. *Am. J. Epidemiol.* 164 (11), 1043–1051.
- Shakeri Yekta, S., Gonsior, M., Schmitt-Kopplin, P., Svensson, B.H., 2012. Characterization of dissolved organic matter in full scale continuous stirred tank biogas reactors using ultrahigh resolution mass spectrometry: a qualitative overview. *Environ. Sci. Technol.* 46 (22), 12711–12719.
- Sleighter, R.L., Hatcher, P.G., 2008. Molecular characterization of dissolved organic matter (DOM) along a river to ocean transect of the lower Chesapeake Bay by ultrahigh resolution electrospray ionization Fourier transform ion cyclotron resonance mass spectrometry. *Mar. Chem.* 110 (3–4), 140–152.
- Spickett, C.M., 2007. Chlorinated lipids and fatty acids: an emerging role in pathology. *Pharmacol. Therapeut.* 115 (3), 400–409.
- Stubbins, A., Spencer, R.G.M., Chen, H., Hatcher, P.G., Mopper, K., Hernes, P.J., Mwamba, V.L., Mangangu, A.M., Wabakanghanzi, J.N., Six, J., 2010. Illuminated darkness: molecular signatures of Congo River dissolved organic matter and its photochemical alteration as revealed by ultrahigh precision mass spectrometry. *Limnol. Oceanogr.* 55, 1467–1477.
- Tak, S., Vellanki, B.P., 2018. Natural organic matter as precursor to disinfection byproducts and its removal using conventional and advanced processes: state of the art review. *J. Water Health* 16 (5), 681–703.
- Timko, S.A., Maydanov, A., Pittelli, S.L., Conte, M.H., Cooper, W.J., Koch, B.P., Schmitt-Kopplin, P., Gonsior, M., 2015. Depth-dependent photodegradation of marine dissolved organic matter. *Front. Marine Sci.* 2.
- Tomlinson, A., Drikas, M., Brookes, J.D., 2016. The role of phytoplankton as precursors for disinfection by-product formation upon chlorination. *Water Res.* 102, 229–240.
- Tseng, L.Y., Gonsior, M., Schmitt-Kopplin, P., Cooper, W.J., Pitt, P., Rosso, D., 2013. Molecular characteristics and differences of effluent organic matter from parallel activated sludge and integrated fixed-film activated sludge (IFAS) processes. *Environ. Sci. Technol.* 47 (18), 10277–10284.
- Tsuji, K., Watanuki, T., Kondo, F., Watanabe, M.F., Nakazawa, H., Suzuki, M., Uchida, H., Harada, K.-I., 1997. Stability of Microcystins from cyanobacteria—iv. effect of chlorination on decomposition. *Toxicon* 35 (7), 1033–1041.
- Tziotis, D., Hertkorn, N., Schmitt-Kopplin, P., 2011. Kendrick-analogous network visualisation of ion cyclotron resonance fourier transform mass spectra: improved options for the assignment of elemental compositions and the classification of organic molecular complexity. *Eur. J. Mass Spectrom.* 17 (4), 415–421.
- van Krevelen, D.W., 1950. Graphical-statistical method for the study of structure and reaction processes of coal. *Fuel* 29, 269–284.
- Voss, R.H., Rapsomatiotis, A., 1985. An improved solvent-extraction based procedure for the gas-chromatographic analysis of resin and fatty-acids in pulp-mill effluents. *J. Chromatogr.* 346 (OCT), 205–214.
- Waterbury, J.B., 1986. Biological and ecological characterization of the marine unicellular cyanobacterium *Synechococcus*. *Photosynthetic Picoplankton* 71–120.
- Wagner, E.D., Hsu, K.-M., Lagunas, A., Mitch, W.A., Plewa, M.J., 2012. Comparative genotoxicity of nitrosamine drinking water disinfection byproducts in Salmonella and mammalian cells. *Mutat. Res. Genet. Toxicol. Environ. Mutagen* 741 (1), 109–115.
- Waller, K., Swan, S.H., DeLorenze, G., Hopkins, B., 1998. Trihalomethanes in drinking water and spontaneous abortion. *Epidemiology* 9 (2), 134–140.
- Wenk, J., Aeschbacher, M., Salhi, E., Canonica, S., von Gunten, U., Sander, M., 2013. Chemical oxidation of dissolved organic matter by chlorine dioxide, chlorine, and ozone: effects on its optical and antioxidant properties. *Environ. Sci. Technol.* 47 (19), 11147–11156.
- Wesén, C., Mu, H., Kvernheim, A.L., Larsson, P., 1992. Identification of chlorinated fatty acids in fish lipids by partitioning studies and by gas chromatography with Hall electrolytic conductivity detection. *J. Chromatogr. A* 625 (2), 257–269.
- Westrick, J.A., Szlag, D.C., Southwell, B.J., Sinclair, J., 2010. A review of cyanobacteria and cyanotoxins removal/inactivation in drinking water treatment. *Analytical and Bioanalytical Chemistry* 397 (5), 1705–1714.
- Winterbourn, C.C., Vandenberg, J.J.M., Roitman, E., Kuypers, F.A., 1992. Chlorohydrin formation from unsaturated fatty-acids reacted with hypochlorous acid. *Arch. Biochem. Biophys.* 296 (2), 547–555.
- Yang, X., Guo, W., Shen, Q., 2011. Formation of disinfection byproducts from chlor(am)ination of algal organic matter. *J. Hazard Mater.* 197, 378–388.
- Yassine, M.M., Harir, M., Dabek-Zlotorzynska, E., Schmitt-Kopplin, P., 2014. Structural characterization of organic aerosol using Fourier transform ion cyclotron resonance mass spectrometry: aromaticity equivalent approach. *Rapid Commun. Mass Spectrom.* 28 (22), 2445–2454.
- Yu, S., Lin, T., Chen, W., Tao, H., 2015. The toxicity of a new disinfection by-product, 2,2-dichloroacetamide (DCAcAm), on adult zebrafish (*Danio rerio*) and its occurrence in the chlorinated drinking water. *Chemosphere* 139 (0), 40–46.
- Zepp, R.G., Sheldon, W.M., Moran, M.A., 2004. Dissolved organic fluorophores in southeastern US coastal waters: correction method for eliminating Rayleigh and Raman scattering peaks in excitation-emission matrices. *Mar. Chem.* 89 (1–4), 15–36.
- Zhai, H., Zhang, X., Zhu, X., Liu, J., Ji, M., 2014. formation of brominated disinfection byproducts during chloramination of drinking water: new polar species and overall kinetics. *Environ. Sci. Technol.* 48 (5), 2579–2588.
- Zhang, H., Zhang, Y., Shi, Q., Zheng, H., Yang, M., 2014. Characterization of unknown brominated disinfection byproducts during chlorination using ultrahigh resolution mass spectrometry. *Environ. Sci. Technol.* 48 (6), 3112–3119.
- Zhang, H.F., Zhang, Y.H., Shi, Q., Hu, J.Y., Chu, M.Q., Yu, J.W., Yang, M., 2012. Study on transformation of natural organic matter in source water during chlorination and its chlorinated products using ultrahigh resolution mass spectrometry. *Environ. Sci. Technol.* 46 (8), 4396–4402.
- Zhang, H.T., Dan, Y.B., Adams, C.D., Shi, H.L., Ma, Y.F., Eichholz, T., 2017. Effect of oxidant demand on the release and degradation of microcystin-LR from *Microcystis aeruginosa* during oxidation. *Chemosphere* 181, 562–568.
- Zhang, T.-Y., Lin, Y.-L., Xu, B., Cheng, T., Xia, S.-J., Chu, W.-H., Gao, N.-Y., 2016. Formation of organic chloramines during chlor(am)ination and UV/chlor(am)ination of algae organic matter in drinking water. *Water Res.* 103, 189–196.
- Zhang, X., Minear, R.A., 2002. Characterization of high molecular weight disinfection byproducts resulting from chlorination of aquatic humic Substances. *Environ. Sci. Technol.* 36 (19), 4033–4038.
- Zhao, Z., Gonsior, M., Luek, J., Timko, S., Ianiri, H., Hertkorn, N., Schmitt-Kopplin, P., Fang, X., Zeng, Q., Jiao, N., Chen, F., 2017. Picocyanobacteria and deep-ocean fluorescent dissolved organic matter share similar optical properties. *Nat. Commun.* 8, 15284.
- Zhu, S.M., Yin, D.D., Gao, N.Y., Zhou, S.Q., Wang, Z.C., Zhang, Z.D., 2016. Adsorption of two microcystins onto activated carbon: equilibrium, kinetic, and influential factors. *Desalination and Water Treatment* 57 (50), 23666–23674.
- Zong, W., Sun, F., Pei, H., Hu, W., Pei, R., 2015. Microcystin-associated disinfection by-products: the real and non-negligible risk to drinking water subject to chlorination. *Chem. Eng. J.* 279, 498–506.